

Contents lists available at [ScienceDirect](http://ScienceDirect)

## Physics Letters B

[www.elsevier.com/locate/physletb](http://www.elsevier.com/locate/physletb)

## Understanding the radiative decays of vector charmonia to light pseudoscalar mesons

Qiang Zhao <sup>a,b,\*</sup><sup>a</sup> Institute of High Energy Physics, Chinese Academy of Sciences, Beijing 100049, PR China<sup>b</sup> Theoretical Physics Center for Science Facilities, CAS, Beijing 100049, PR China

## ARTICLE INFO

## Article history:

Received 12 December 2010

Received in revised form 17 January 2011

Accepted 23 January 2011

Available online 27 January 2011

Editor: J.-P. Blaizot

## Keywords:

Charmonium radiative decays

Vector meson dominance

Charmonium hadronic decays

## ABSTRACT

We show that the newly measured branching ratios of vector charmonia ( $J/\psi$ ,  $\psi'$  and  $\psi(3770)$ ) into  $\gamma P$ , where  $P$  stands for light pseudoscalar mesons  $\pi^0$ ,  $\eta$ , and  $\eta'$ , can be well understood in the framework of vector meson dominance (VMD) in association with the  $\eta_c$ – $\eta(\eta')$  mixings due to the axial gluonic anomaly. These two mechanisms behave differently in  $J/\psi$  and  $\psi' \rightarrow \gamma P$ . A coherent understanding of the branching ratio patterns observed in  $J/\psi(\psi') \rightarrow \gamma P$  can be achieved by self-consistently including those transition mechanisms at hadronic level. The branching ratios for  $\psi(3770) \rightarrow \gamma P$  are predicted to be rather small.

© 2011 Elsevier B.V. Open access under [CC BY license](http://creativecommons.org/licenses/by/3.0/).

## 1. Introduction

The recent measurements of the vector charmonium radiative decays to light pseudoscalars, i.e.  $J/\psi$ ,  $\psi'$  and  $\psi(3770) \rightarrow \gamma\pi^0$ ,  $\gamma\eta$  and  $\gamma\eta'$ , have brought surprises and interests to us. Earlier, the CLEO Collaboration [1] renewed the branching ratios for  $J/\psi \rightarrow \gamma\pi^0$ ,  $\gamma\eta$ ,  $\gamma\eta'$ , and  $\psi' \rightarrow \gamma\eta'$ , which are consistent with the averages from 2008 Particle Data Group [2]. The branching ratio upper limits for  $\psi' \rightarrow \gamma\pi^0$  and  $\gamma\eta$  were set, which were more than one order of magnitude smaller than that for  $\psi' \rightarrow \gamma\eta'$ . Meanwhile, the upper limits for  $\psi(3770) \rightarrow \gamma P$ , where  $P$  stands for pseudoscalar  $\pi^0$ ,  $\eta$  and  $\eta'$ , were set to be about  $10^{-5} \sim 10^{-6}$ . The  $\psi'$  radiative decays are also investigated by the BESIII Collaboration with the newly collected 106 million  $\psi'$  events, and the results turn out to be tantalizing. It shows that the branching ratios for  $\psi' \rightarrow \gamma\pi^0$  and  $\gamma\eta$  are only at an order of  $10^{-6}$ , which are nearly two orders of magnitude smaller than  $\psi' \rightarrow \gamma\eta'$  [3].

The mysterious aspects somehow are correlated with the  $J/\psi$  and  $\psi'$  data. It is found that the branching ratio for  $J/\psi \rightarrow \gamma\pi^0$  is much smaller than those for  $J/\psi \rightarrow \gamma\eta$  and  $\gamma\eta'$  [2,4]. This could be a consequence of suppressions of gluon couplings to isovector currents. As a comparison, the observation in  $\psi' \rightarrow \gamma P$  is indeed puzzling. The immediate question is, what drives the difference of decay patterns between  $J/\psi$  and  $\psi'$ .

In the literature, the radiative decays of the vector charmonia attracted a lot of theoretical efforts. An early study by the QCD sum rules [5] suggested the dominance of short-distance  $c\bar{c}$  annihilations. The gluon and  $q\bar{q}$  transition matrix elements were computed by coupling the gluon fields to the pseudoscalar states with which the branching ratio fraction  $BR(J/\psi \rightarrow \gamma\eta')/BR(J/\psi \rightarrow \gamma\eta)$  was satisfactorily described. In Ref. [6], the  $\eta_c$  mixings with the light pseudoscalars  $\eta$  and  $\eta'$  were extracted through the axial gluonic anomaly on the basis of chiral and large  $N_c$  approach. By assuming that the partial widths of  $J/\psi \rightarrow \gamma\eta$  and  $\gamma\eta'$  were saturated by the  $\eta_c$ – $\eta(\eta')$  mixing, the branching ratios for  $J/\psi \rightarrow \gamma\eta$  and  $\gamma\eta'$  were accounted for to the correct orders of magnitude. This issue was revisited by Feldmann et al. who proposed to extract the mixing and decay constants on the quark flavor basis [7]. This scheme can be easily extended to accommodate the mixing of  $\eta_c$  with  $\eta$  and  $\eta'$  from which the  $\eta_c$ – $\eta(\eta')$  mixing angles were extracted and turned out to be consistent with those from Refs. [6,8,9].

Interestingly, the new data from BESIII for  $\psi' \rightarrow \gamma P$  seem to suggest a deviation from the saturation assumption. It implies that some other mechanisms become important in  $\psi' \rightarrow \gamma P$ , although they may not play a significant role in  $J/\psi \rightarrow \gamma P$ . In this work, we shall show that the vector meson dominance (VMD) model is an ideal framework to make a coherent analysis of the  $\eta_c$ – $\eta(\eta')$  mixing effects and contributions from intermediate vector mesons. We shall show that the  $\psi' \rightarrow \gamma P$  is not saturated by the  $\eta_c$ – $\eta(\eta')$  mixing. Instead, one important mechanism that drives the difference between  $J/\psi$  and  $\psi' \rightarrow \gamma P$  and produces the observed patterns is the sizeable coupling of  $\psi' \rightarrow J/\psi P$ .

\* Address for correspondence: Institute of High Energy Physics, Chinese Academy of Sciences, Beijing 100049, PR China.

E-mail address: [zhaoq@ihep.ac.cn](mailto:zhaoq@ihep.ac.cn).

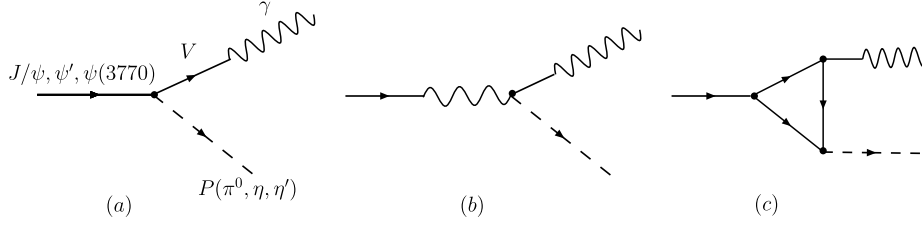


Fig. 1. Schematic diagrams for  $J/\psi(\psi', \psi(3770)) \rightarrow \gamma P$  in the frame of VMD.

As follows, we first give a brief introduction to the VMD model and lay out the correlated aspects of the  $\eta_c$ – $\eta(\eta')$  mixings in Section 2. The detailed analysis, calculation results and discussions will then be presented in Section 3. A brief summary will be given in Section 4.

## 2. VMD model and $\eta_c$ – $\eta(\eta')$ mixings

In the VMD model (e.g. see review of Refs. [10,11]) the electromagnetic (EM) current can be decomposed into a sum of all neutral vector meson fields including both isospin-0 and isospin-1 components. The leading  $V\gamma^*$  effective coupling can be written as:

$$\mathcal{L}_{V\gamma} = \sum_V \frac{eM_V^2}{f_V} V_\mu A^\mu, \quad (1)$$

where  $V^\mu (= \rho, \omega, \phi, J/\psi, \dots)$  denotes the vector meson field. The photon–vector-meson coupling constant  $eM_V^2/f_V$  can be extracted from the partial decay width  $\Gamma_{V \rightarrow e^+e^-}$ . Neglecting the mass of electron and positron, we have

$$\frac{e}{f_V} = \left[ \frac{3\Gamma_{V \rightarrow e^+e^-}}{2\alpha_e |\mathbf{p}_e|} \right]^{1/2}, \quad (2)$$

where  $\mathbf{p}_e$  is the electron three-vector momentum in the vector meson rest frame, and  $\alpha_e$  is the EM fine-structure constant.

For the decays of  $J/\psi(\psi', \psi(3770)) \rightarrow \gamma P$ , the VMD contributing diagrams are illustrated in Fig. 1. This classification is based on the photon producing mechanisms and related to the experimental measurements. For instance, Fig. 1(a) identifies such a process that the photon is connected to a hadronic vector meson fields. It requires a sum over all strong transitions of  $J/\psi(\psi', \psi(3770)) \rightarrow VP$  channels.

The second process in Fig. 1(b) is via charmonium electromagnetic (EM) annihilations. Such a process generally has small contributions in comparison with the strong transitions. However, it is likely that the EM amplitudes may have significant effects in some exclusive decay channels. In recent series studies [12–15] it shows that in the hadronic decays of  $J/\psi(\psi') \rightarrow VP$ , the short (via three gluon annihilation) and long-distance (Fig. 1(c)) transition amplitudes may have a destructive interfering mode that would efficiently reduce the strong transition amplitudes in some exclusive channels. As a consequence, the EM amplitudes may become compatible with the strong ones, and manifest themselves in experimental observables. This issue is related to the so-called “ $\rho\pi$  puzzle”, which questions why the branching ratio fraction  $BR(\psi' \rightarrow \rho\pi)/BR(J/\psi \rightarrow \rho\pi)$  is so strongly suppressed in comparison with the pQCD expectation values [16–18]. A review of this subject and some recent progresses on this problem can be found in the literature [12,19,20].

In the present work, our attention is to understand whether the data for  $J/\psi(\psi', \psi(3770)) \rightarrow \gamma P$  are consistent with those for  $J/\psi(\psi', \psi(3770)) \rightarrow VP$ , and what drives the different radiative decay patterns between  $J/\psi$  and  $\psi'$ . We shall adopt the available experimental measurements of  $J/\psi(\psi', \psi(3770)) \rightarrow VP$

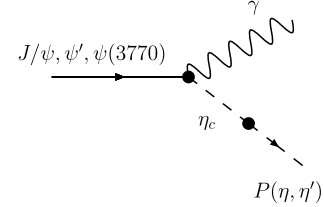


Fig. 2. Schematic diagram for  $J/\psi(\psi', \psi(3770)) \rightarrow \gamma\eta$  and  $\gamma\eta'$  via  $\eta_c$ – $\eta(\eta')$  mixing.

in the calculations of the VMD contributions. This means we need not worry about the detailed transition mechanisms for  $J/\psi(\psi', \psi(3770)) \rightarrow VP$  at this moment. Also, by adopting the experimental data for  $J/\psi(\psi', \psi(3770)) \rightarrow VP$ , we need not consider the  $\eta$ – $\eta'$  mixing processes since they have been contained in the data for  $J/\psi(\psi', \psi(3770)) \rightarrow VP$ .

It is worth noting in advance another feature with this classification of Fig. 1. Namely, transitions between vector charmonia may also contribute. For instance,  $\psi' \rightarrow J/\psi\eta$  will contribute to  $\psi' \rightarrow \gamma\eta$ . We will show later that this process is essential for understanding the radiative decay patterns for  $J/\psi$  and  $\psi' \rightarrow \gamma P$ .

Apart from the transitions via Fig. 1, another important transition is via Fig. 2 which corresponds to the  $\eta_c$ – $\eta(\eta')$  mixing due to the axial vector anomaly. Note that the process of Fig. 1(a) with an intermediate charmonium does not overlap with Fig. 2 at the hadronic level. In fact, it is interesting to note their correlated features:

- (i) In both cases, the  $c\bar{c}$  annihilate at short distances. In Fig. 1(a), the vector configuration of  $c\bar{c}$  annihilates into a photon, i.e.  $c\bar{c}$  in a relative S-wave with spin-1, while in Fig. 2 the pseudoscalar  $c\bar{c}$  are in a relative S-wave but with spin-0, and then annihilates into gluons.
- (ii) The process of Fig. 2 is through a typical magnetic dipole (M1) transition of  $J/\psi(\psi', \psi(3770)) \rightarrow \gamma\eta_c$ , which can be regarded as a non-vector-resonance contribution in respect to the VMD scenario.

With the Lagrangian of Eq. (1), the transition amplitude can be expressed as

$$\mathcal{M}_{\gamma P}^{\text{VMD}} = \left( \sum_V \frac{1}{p_V^2 - M_V^2} \frac{eM_V^2}{f_V} g_{\psi VP} \right) \mathcal{F}(\mathbf{p}_V^2) \epsilon_{\mu\nu\alpha\beta} P_\psi^\mu \epsilon_\psi^\nu p_V^\alpha \epsilon_V^\beta, \quad (3)$$

where  $g_{\psi VP}$  denotes the coupling constants for the hadronic vertex of  $J/\psi(\psi', \psi(3770)) \rightarrow VP$ , and will be determined by experimental data via

$$\mathcal{M}_{VP} = g_{\psi VP} \mathcal{F}(\mathbf{p}_V^2) \epsilon_{\mu\nu\alpha\beta} P_\psi^\mu \epsilon_\psi^\nu p_V^\alpha \epsilon_V^\beta. \quad (4)$$

We adopt an empirical form for the form factor [21–23]:

$$\mathcal{F}(\mathbf{p}^2) \equiv e^{-\mathbf{p}^2/8\beta^2}, \quad (5)$$

where parameter  $\beta$  is in a range of 300–500 MeV. This form factor can be interpreted as the wavefunction overlap which would be suppressed in a large recoil momentum region for the final state particles [21–23]. The invariant form factor can also be regarded reasonable in this case. The decay processes are treated in the c.m. frame of the initial meson. Therefore, the anti-symmetric tensor structure of the interactions can always be reduced to a form of  $M_\psi \epsilon_\psi \cdot (\mathbf{p}_V \times \epsilon_V)$ , which explicitly depends on the three-vector momentum of the final state vector meson. Note that for the anti-symmetric tensor couplings all the contributions to the transition amplitude can be absorbed into the effective coupling form factor. Because of this, it is natural to expect that the form factor would contain information of meson wavefunction overlaps with an explicit three-vector-momentum dependence. In particular, a harmonic oscillator potential for the quark–antiquark system will lead to a form factor similar to Eq. (5).

We shall determine the form factor parameter  $\beta$  combining the data for  $J/\psi(\psi') \rightarrow VP$  and  $\gamma P$ . It will then be fixed and adopted for the calculations of other channels. In the transition of Fig. 1(a), the vector meson will carry the momentum of the final state photon  $\mathbf{p}_\gamma$ .

The transition amplitudes of Fig. 2 can be expressed as

$$\begin{aligned} \mathcal{M}_{\gamma P}^{\text{mixing}} &= \lambda_{P\eta_c} g_{\psi\gamma\eta_c} \epsilon_{\mu\nu\alpha\beta} P_\psi^\mu \epsilon_\psi^\nu p_\gamma^\alpha \epsilon_\gamma^\beta \\ &\equiv \tilde{\lambda}_{P\eta_c} \mathcal{F}(\mathbf{p}_\gamma^2) \epsilon_{\mu\nu\alpha\beta} P_\psi^\mu \epsilon_\psi^\nu p_\gamma^\alpha \epsilon_\gamma^\beta, \end{aligned} \quad (6)$$

where  $\lambda_{P\eta_c}$  is the mixing angle between pseudoscalar  $P$  and  $\eta_c$ . It has been extracted in Ref. [6],  $\lambda_{\eta\eta_c} = -4.6 \times 10^{-3}$  and  $\lambda_{\eta'\eta_c} = -1.2 \times 10^{-2}$ , which are also obtained by Ref. [7]. It should be noted that in the above equation the coupling  $g_{\psi\gamma\eta_c}$  is extracted from the data for  $J/\psi(\psi') \rightarrow \gamma\eta_c$ . The non-local effects from the off-shell  $\eta_c$  at the mass of  $\eta(\eta')$  have been included in the mixing angles [6]. In the second line, we define a reduced coupling  $\tilde{\lambda}_{P\eta_c} \equiv \lambda_{P\eta_c} g_{\psi\gamma\eta_c} / \mathcal{F}(\mathbf{p}_\gamma^2)$ , which can be directly compared with the effective coupling  $(e/f_V) g_{\psi VP}$  in Eq. (3).

We do not include the  $\eta'_c$  mixings with the  $\eta(\eta')$  in  $J/\psi \rightarrow \gamma\eta$  and  $\gamma\eta'$  since their mixing angles are relatively small. Nevertheless, the  $\eta'_c$  mixing effects will be further suppressed by the unknown but believe-to-be-small branching ratio for  $\eta'_c \rightarrow J/\psi\gamma$ .

### 3. Numerical results

#### 3.1. Results from VMD

In Table 1, the data for  $J/\psi$ ,  $\psi'$  and  $\psi(3770) \rightarrow VP$  from PDG 2010 [4] are listed. It shows that most of the light  $VP$  channels have been measured for  $J/\psi$  and  $\psi'$  hadronic decays. In contrast, most of the light  $VP$  channels for  $\psi(3770)$  are below the experimental precision limit except for  $\phi\eta$ . As mentioned earlier, the  $J/\psi(\psi') \rightarrow VP$  channels are correlated with the so-called “ $\rho\pi$  puzzle” in the literature. However, our attention in the present work is different. We shall use the experimental data for  $J/\psi(\psi', \psi(3770)) \rightarrow VP$  as an input to investigate the role played by the VMD mechanisms in the vector charmonium radiative decays. This treatment means that one need not be concerned about the detailed transition mechanisms for  $J/\psi(\psi', \psi(3770)) \rightarrow VP$  at this moment since they all have been contained in the experimental data. We emphasize that this should not be a trivial starting point. Success of such a prescription would help us clarify two major processes in the charmonium radiative decays, i.e. the relative  $S$ -wave  $c\bar{c}$  annihilations would occur either via spin-1 or spin-0 configurations.

In Table 1, the branching ratios for  $\psi'$  and  $\psi(3770) \rightarrow J/\psi\eta$  and  $J/\psi\pi^0$  are also listed. As pointed out earlier, these chan-

**Table 1**

Branching ratios for  $J/\psi(\psi', \psi(3770)) \rightarrow VP$  from PDG 2010 [4]. The dash “–” and dots “...” denote the forbidden and unavailable channels, respectively.

Channels	$J/\psi$	$\psi'$	$\psi(3770)$
$J/\psi\pi^0$	–	$(1.30 \pm 0.10) \times 10^{-3}$	$< 2.8 \times 10^{-4}$
$J/\psi\eta$	–	$(3.28 \pm 0.07)\%$	$(9 \pm 4) \times 10^{-4}$
$\rho\pi$	$(1.69 \pm 0.15)\%$	$(3.2 \pm 1.2) \times 10^{-5}$	–
$\rho^0\pi^0$	$(5.6 \pm 0.7) \times 10^{-3}$	...	–
$\omega\pi^0$	$(4.5 \pm 0.5) \times 10^{-4}$	$(2.1 \pm 0.6) \times 10^{-5}$	–
$\phi\pi^0$	$< 6.4 \times 10^{-6}$	$< 4 \times 10^{-6}$	–
$\omega\eta$	$(1.74 \pm 0.20) \times 10^{-3}$	$< 1.1 \times 10^{-5}$	–
$\phi\eta$	$(7.5 \pm 0.8) \times 10^{-4}$	$(2.8^{+1.0}_{-0.8}) \times 10^{-5}$	$(3.1 \pm 0.7) \times 10^{-4}$
$\rho\eta$	$(1.93 \pm 0.23) \times 10^{-4}$	$(2.2 \pm 0.6) \times 10^{-5}$	–
$\omega\eta'$	$(1.82 \pm 0.21) \times 10^{-4}$	$(3.2^{+2.5}_{-2.1}) \times 10^{-5}$	–
$\phi\eta'$	$(4.0 \pm 0.7) \times 10^{-4}$	$(4.1 \pm 1.6) \times 10^{-5}$	–
$\rho\eta'$	$(1.05 \pm 0.18) \times 10^{-4}$	$(1.9^{+1.7}_{-1.2}) \times 10^{-5}$	–

**Table 2**

Effective couplings  $\frac{e}{f_V} g_{\psi VP}$  (in unit of  $\text{GeV}^{-1}$ ) for  $J/\psi(\psi', \psi(3770)) \rightarrow \gamma P$  extracted from the intermediate  $VP$  channels. Note that the form factor  $\mathcal{F}(\mathbf{p}_\gamma^2)$  is not included. The dash “–” and dots “...” denote the forbidden and unavailable channels, respectively.

$VP$	$(e/f_V) g_{J/\psi VP}$	$(e/f_V) g_{\psi' VP}$	$(e/f_V) g_{\psi(3770) VP}$
$J/\psi\pi^0$	–	$4.02 \times 10^{-4}$	$< 9.73 \times 10^{-4}$
$J/\psi\eta$	–	$6.25 \times 10^{-3}$	$2.74 \times 10^{-3}$
$J/\psi\eta'$	–	$3.01 \times 10^{-2}$	$1.32 \times 10^{-2}$
$\psi'\pi^0$	$2.40 \times 10^{-4}$	–	–
$\psi'\eta$	$3.74 \times 10^{-3}$	–	–
$\psi'\eta'$	$1.80 \times 10^{-2}$	–	–
$\psi(3770)\pi^0$	$< 3.22 \times 10^{-4}$	–	–
$\psi(3770)\eta$	$9.09 \times 10^{-4}$	–	–
$\psi(3770)\eta'$	$4.37 \times 10^{-3}$	–	–
$\rho^0\pi^0$	$2.83 \times 10^{-3}$	$6.69 \times 10^{-4}$	...
$\omega\pi^0$	$2.35 \times 10^{-4}$	$2.73 \times 10^{-4}$	...
$\phi\pi^0$	$< 2.51 \times 10^{-5}$	$< 1.02 \times 10^{-4}$	...
$\omega\eta$	$3.97 \times 10^{-4}$	$< 1.67 \times 10^{-4}$	...
$\phi\eta$	$2.72 \times 10^{-4}$	$2.69 \times 10^{-4}$	$1.02 \times 10^{-2}$
$\rho\eta$	$4.52 \times 10^{-4}$	$8.10 \times 10^{-4}$	...
$\omega\eta'$	$9.54 \times 10^{-5}$	$2.02 \times 10^{-4}$	...
$\phi\eta'$	$1.48 \times 10^{-4}$	$1.20 \times 10^{-4}$	...
$\rho\eta'$	$2.48 \times 10^{-4}$	$5.34 \times 10^{-4}$	...

nels are rather important for understanding the observed branching ratio patterns. The effective coupling  $g_{\psi VP}$  in Eqs. (3) and (4) is a scale-independent constant. The data in Table 1 will allow us to extract  $g_{\psi VP}$  for different  $VP$  channels in association with the form factor parameter  $\beta$ . The overall numerical study suggests that a smaller value of  $\beta = 0.3 \text{ GeV}$  is favored. This is due to that in  $J/\psi(\psi') \rightarrow \gamma P$ , the intermediate vector mesons are in a highly virtual kinematic region. Part of the off-shell effects would be absorbed into the form factor parameter  $\beta$  as we adopt the  $V \rightarrow \gamma^*$  couplings  $e/f_V$  which are determined by data for  $V \rightarrow e^+e^-$  [4].

In Table 2 we list the joint coupling constants  $(e/f_V) g_{\psi VP}$  for different  $VP$  channels as a reference. These quantities are the corresponding scale-independent couplings in  $J/\psi(\psi') \rightarrow \gamma P$ , and provide an immediate estimate of the relative strengths among those transitions amplitudes that involve different vector mesons. The form factor  $\mathcal{F}(\mathbf{p}_\gamma^2) = e^{-\mathbf{p}_\gamma^2/8\beta^2}$  with  $\beta = 0.3 \text{ GeV}$  will lead to an overall suppression to the vertices. In the light  $VP$  sector, the strong  $\rho^0\gamma$  coupling accounts for the relatively large contributions from the  $\rho^0$  mediated transitions.

In the vector-charmonium-mediated channels, the non-negligible coupling of  $g_{\psi' J/\psi\eta}$  implies a non-vanishing coupling of  $g_{\psi' J/\psi\eta'}$ , although the decay of  $\psi' \rightarrow J/\psi\eta'$  is prohibited by the phase space. The influence of  $\psi' \rightarrow J/\psi\eta'$  in  $\psi' \rightarrow \gamma\eta'$  should

not be neglected and must be included in the amplitude. As we know, the  $\eta$  and  $\eta'$  can be expressed as mixtures of quark flavor singlets:

$$\begin{aligned}\eta &= \cos \alpha_P n\bar{n} - \sin \alpha_P s\bar{s}, \\ \eta' &= \sin \alpha_P n\bar{n} + \cos \alpha_P s\bar{s},\end{aligned}\quad (7)$$

where  $\alpha_P \equiv \arctan \sqrt{2} + \theta_P$ , and  $\theta_P \simeq -11.7^\circ$  is the SU(3) flavor singlet and octet mixing angle. Thus, we have

$$g_{\psi' J/\psi \eta'} = g_{\psi' J/\psi \eta} \left( \frac{\sqrt{2} \sin \alpha_P + R \cos \alpha_P}{\sqrt{2} \cos \alpha_P - R \sin \alpha_P} \right), \quad (8)$$

where  $R$  describes the SU(3) flavor symmetry breaking. In general,  $R \equiv f_\pi/f_K \simeq 0.838$  is commonly adopted for the relative production strength of an  $s\bar{s}$  to  $q\bar{q}$ . The above relation is based on the  $q\bar{q}$  and  $s\bar{s}$  mixing scheme [12,24–27] and does not include a possible glueball component. If one extends the  $\eta$ – $\eta'$  mixing to accommodate the glueball  $\mathcal{G}$ , the coupling of  $g_{\psi' J/\psi \eta'}$  can be expressed as

$$g_{\psi' J/\psi \eta'} = g_{\psi' J/\psi \eta} \left( \frac{\sqrt{2} X_{\eta'} + R Y_{\eta'} + G Z_{\eta'}}{\sqrt{2} X_\eta + R Y_\eta + G Z_\eta} \right), \quad (9)$$

where parameter  $G$  denotes the relative strength of producing the pseudoscalar glueball  $\mathcal{G}$  to a light  $q\bar{q}$  component. The general flavor wavefunctions for  $\eta$  and  $\eta'$  are

$$\begin{aligned}\eta &= X_\eta n\bar{n} + Y_\eta s\bar{s} + Z_\eta \mathcal{G}, \\ \eta' &= X_{\eta'} n\bar{n} + Y_{\eta'} s\bar{s} + Z_{\eta'} \mathcal{G},\end{aligned}\quad (10)$$

for which different model solutions can be found in the literature [12,24–26,28]. Generally speaking, the introduction of the glueball component will introduce new parameters. Taking into account that the glueball components within the  $\eta$  and  $\eta'$  are rather small, and Eq. (7) is well established to leading accuracy, we neglect the possible glueball mixing effects in the present analysis.

We adopt the same on-shell couplings of  $g_{J/\psi \psi' P}$  as those extracted in  $\psi' \rightarrow J/\psi P$  since the kinematics for these two processes are similar to each other. Namely, we neglect the off-shell effects with the couplings of  $g_{J/\psi \psi' P}$  in contrast with  $g_{\psi' J/\psi P}$ .

As listed in Table 2, it shows that the charmonium poles are one of the most important contributing sources to the  $J/\psi(\psi') \rightarrow \gamma\eta$  and  $\gamma\eta'$ , which seems to be slightly out of expectation and has not been addressed before. This feature is explicit for the  $\psi'$  decays since the decay of  $\psi' \rightarrow J/\psi\eta$  is experimentally accessible. In contrast, other  $VP$  channels' contributions to  $\gamma P$  are rather small due to their relatively small branching ratios. Similar phenomena appear in  $J/\psi \rightarrow VP$  except that the sizeable branching ratio for

$J/\psi \rightarrow \rho\pi$  would also make the  $\rho\pi$  channel an important contributor to the  $\gamma P$  amplitude.

### 3.2. Results from $\eta_c$ – $\eta(\eta')$ mixings

In Table 3, we list the effective couplings derived from the  $\eta_c$ – $\eta(\eta')$  mixings [6]. These values can be directly compared with  $(e/f_V)g_{\psi VP}$  listed in Table 2. It shows that in  $J/\psi \rightarrow \gamma\eta$  and  $\gamma\eta'$ , the axial-anomaly-driving mixing contributions turn out to be more predominant than the VMD, while in  $\psi' \rightarrow \gamma P$  the most important contribution is from the  $J/\psi$  pole.

We list the individual branching ratios given by the VMD and  $\eta_c$ – $\eta(\eta')$  mixings in Table 4 as a comparison. Indeed, it shows that the mixing contributions have nearly saturated the branching ratios in  $J/\psi \rightarrow \gamma\eta$  and  $\gamma\eta'$ . However, the situation changes in  $\psi'$  decays where the VMD mechanisms become more important. An interesting feature is that one in principle needs both to give an overall account of the measured branching ratios.

Note that in Table 4, the ranges of uncertainties for the VMD results are given by the experimental errors in Table 1.

### 3.3. Discussions

To compare with the experimental measurements, we need to add the VMD and  $\eta_c$ – $\eta(\eta')$  mixing amplitudes to each other coherently. Taking the advantage of the unique Lorentz structure of the  $VVP$  coupling, we can express the total transition amplitude as follows,

$$\mathcal{M}_{\text{tot}} = \mathcal{M}_{\gamma P}^{\text{VMD}} + e^{i\delta} \mathcal{M}_{\gamma P}^{\text{mixing}}, \quad (11)$$

where  $\delta$  is introduced to take into account possible phase differences between these two amplitudes. In the transition processes that we are interested in here, such a phase ambiguity seems inevitable due to a important role played by hadronic transition mechanisms. Since several different hadronic level amplitudes are involved in  $\mathcal{M}_{\gamma P}^{\text{VMD}}$ , it is not a necessity that  $\mathcal{M}_{\gamma P}^{\text{VMD}}$  and  $\mathcal{M}_{\gamma P}^{\text{mixing}}$  should share the same phase angle for different pseudoscalar channels. We expect that the experimental data [3,4] would provide a constraint on it.

In Fig. 3, we plot the  $\delta$ -dependence of the branching ratios in comparison with the PDG 2010 averages [4] and new experimental data from BESIII [3]. It shows that in the two decays,  $J/\psi \rightarrow \gamma\eta$  and  $\psi' \rightarrow \gamma\eta'$ , the transition amplitudes of the VMD and  $\eta_c$ – $\eta(\eta')$  mixings are well in phase. In contrast, they seem to be out of phase in  $\psi' \rightarrow \gamma\eta$ , although the experimental uncertainties are quite large. The central value of the data can be best accounted for at  $\delta \simeq 140^\circ$  or  $220^\circ$ . More complex phases appear in  $J/\psi \rightarrow \gamma\eta'$ , although the dominant contributions are from the axial gluonic anomaly. In this case, the phase angle  $\delta = 80^\circ$  or  $280^\circ$  are favored. It should be mentioned that in a recent paper by BESIII [29], a smaller branching ratio for  $J/\psi \rightarrow \gamma\eta'$  is reported, i.e.  $BR(J/\psi \rightarrow \gamma\eta') = (4.86 \pm 0.03 \pm 0.24) \times 10^{-3}$ . This value is consistent with the PDG 2010 average, and would favor  $\delta \simeq 90^\circ$  or  $270^\circ$ .

In Table 5, we list the coherent results for the branching ratios  $BR(J/\psi \rightarrow \gamma P)$  and  $BR(\psi' \rightarrow \gamma P)$  in comparison with the data

**Table 3**  
Reduced effective couplings (in unit of  $\text{GeV}^{-1}$ ) from the  $\eta_c$ – $\eta(\eta')$  mixings.

	$\tilde{\lambda}_{P\eta_c}(J/\psi \rightarrow \gamma P)$	$\tilde{\lambda}_{P\eta_c}(\psi' \rightarrow \gamma P)$
$\gamma\eta$	$2.10 \times 10^{-2}$	$5.12 \times 10^{-3}$
$\gamma\eta'$	$3.66 \times 10^{-2}$	$8.91 \times 10^{-3}$

**Table 4**  
Branching ratios for  $J/\psi(\psi') \rightarrow \gamma\eta$  and  $\gamma\eta'$  given by the VMD mechanisms and  $\eta_c$ – $\eta(\eta')$  mixings, respectively.

$\gamma P$	$J/\psi \rightarrow \gamma P$		$\psi' \rightarrow \gamma P$	
	VMD	$\eta_c$ mixing	VMD	$\eta_c$ mixing
$\gamma\pi^0$	$(1.64 \sim 2.04) \times 10^{-5}$	–	$(0.66 \sim 1.15) \times 10^{-7}$	–
$\gamma\eta$	$(0.060 \sim 0.063) \times 10^{-3}$	$0.61 \times 10^{-3}$	$(3.33 \sim 3.61) \times 10^{-6}$	$1.62 \times 10^{-6}$
$\gamma\eta'$	$(1.04 \sim 1.05) \times 10^{-3}$	$3.50 \times 10^{-3}$	$(0.58 \sim 0.61) \times 10^{-4}$	$0.096 \times 10^{-4}$



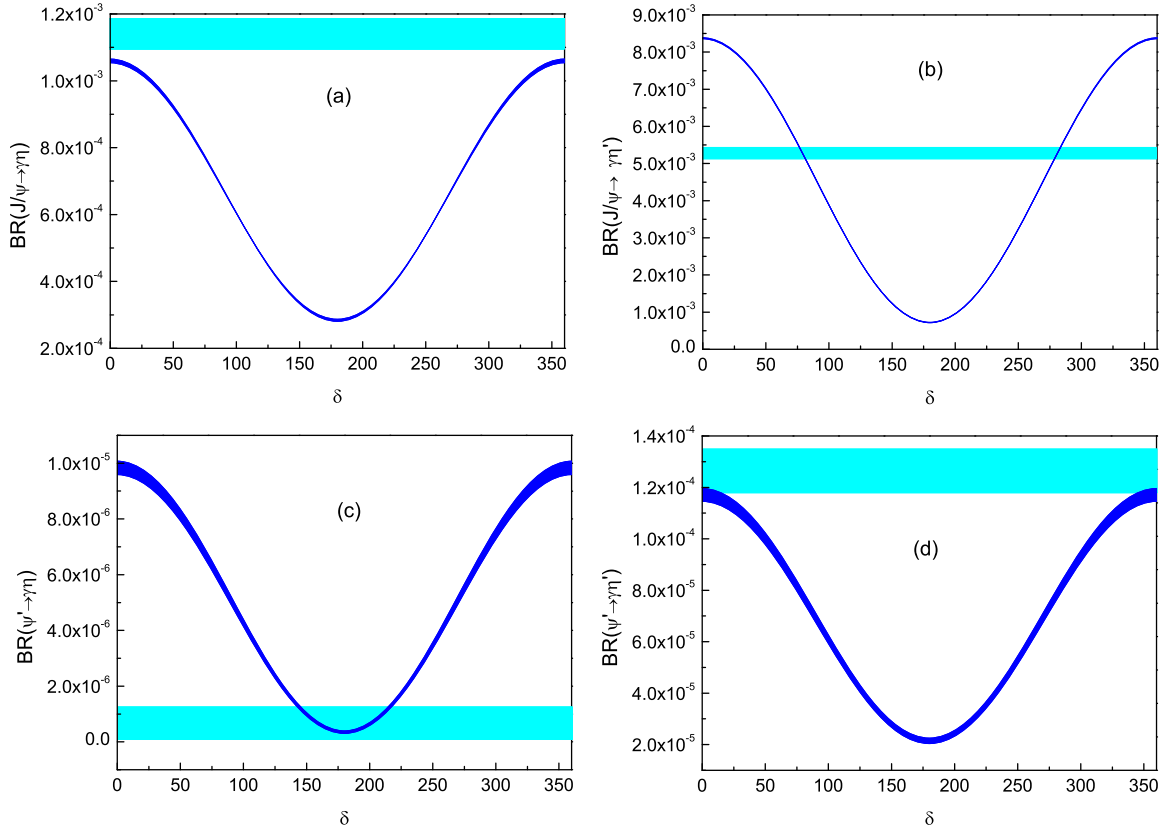


**Fig. 3.** The phase angle  $\delta$ -dependence of branching ratios for  $J/\psi \rightarrow \gamma\eta^{(\prime)}$  ((a) and (b)) and  $\psi' \rightarrow \gamma\eta^{(\prime)}$  ((c) and (d)). The experimental data with uncertainties are shown as the straight bands, while the theoretical results are shown by the curvilinear bands. The theory uncertainties are given by the uncertainties of the data for  $J/\psi(\psi') \rightarrow VP$  as listed in Table 1.

again [3,4]. The phase angles are fixed as shown in Fig. 3 with the best description of the central value of the data. Again, the theoretical uncertainties due to adopting the data for  $J/\psi(\psi') \rightarrow VP$  are included. We also include the  $\psi(3770) \rightarrow \gamma P$  as a prediction of the VMD mechanism. The predicted branching ratios are all small. The  $\eta_c$  mixing contributions are not included here due to lack of data. Also, most of the light vector meson contributions to the  $\psi(3770)$  radiative decays are rather small and unavailable. Thus, the predicted branching ratios are actually given by the  $J/\psi$  pole in the VMD model. Given the same statistics for  $\psi(3770)$  as the  $\psi'$  from BESIII, the accessible channel would be  $\psi(3770) \rightarrow \gamma\eta'$ . Experimental examination of the predicted pattern in Table 5 would be an interesting test of the VMD mechanisms proposed in this work.

In general, the results fit the observed branching ratio pattern very well, except that the branching ratio for  $\psi' \rightarrow \gamma\pi^0$  seems to have some discrepancies. It might be a sign that other non-VMD mechanisms may also play a role. For  $J/\psi \rightarrow \gamma\pi^0$ , the dominance of  $J/\psi \rightarrow \rho^0\pi^0$  can naturally account for the data. It should be mentioned that Ref. [30] also confirms the VMD contributions via the  $\rho^0\pi^0$  channel to  $J/\psi \rightarrow \gamma\pi^0$ .

Our investigation suggests the importance of a coherent treatment for the VMD mechanism and  $\eta_c$ - $\eta(\eta')$  mixings. Note that the charmonium pole contribution has not been included by the previous studies [5–9,24,28]. Meanwhile, an understanding of why the VMD and axial gluonic anomaly mechanisms play different roles in  $J/\psi$  and  $\psi'$  decays would be essentially important. The following points may help to clarify this question:

(i) As mentioned earlier, there are some interesting correspondences between the axial gluonic anomaly and VMD in this

case. In the axial gluonic anomaly transitions the  $c\bar{c}$  annihilate into gluon fields at short distances in a relative S-wave and spin-0, which induces mixings with the Goldstone boson  $\eta$  and SU(3) flavor singlet  $\eta'$ . The photon radiation can be regarded as from non-vector-resonance M1 transitions. In the VMD transitions via the charmonium state, the  $c\bar{c}$  also annihilate at short distances in a relative S-wave, but with spin-1. In this case, the annihilated  $c\bar{c}$  couple to a photon, and radiate two soft gluons which can couple to pseudoscalar states.

(ii) The difference between those two mechanisms can be well-understood quantum mechanically. For  $J/\psi \rightarrow \gamma\eta^{(\prime)}$ , the VMD transitions via  $\psi'$  pole is relative suppressed by the  $\psi'\gamma$  coupling since as the first radial excited state the wavefunction of  $\psi'$  at the origin is smaller than that of  $J/\psi$ . In contrast, the axial-gluonic-anomaly-driving  $\eta_c$ - $\eta(\eta')$  mixings will occur via  $J/\psi \rightarrow \gamma\eta_c \rightarrow \gamma\eta^{(\prime)}$ , where the first step is a typical EM M1 transition between two ground charmonium states. It is allowed by the quantum transition selection rule at leading order.

The situation changes in  $\psi' \rightarrow \gamma\eta^{(\prime)}$ . On the one hand, the VMD transition will be dominated by the  $J/\psi$  pole, which will be coupled to the EM field. On the other hand, the axial gluonic anomaly transitions via the  $\psi'$ - $\eta_c$  M1 transition will be suppressed by the quantum transition selection rule at leading order. For the  $\eta'_c$ -mediated transition, the  $\eta'_c$  mixings with the  $\eta$  and  $\eta'$  will then be suppressed [6].

The above qualitative argument explains why the VMD mechanism and axial gluonic anomaly play different roles in  $J/\psi$  and  $\psi'$  decays, respectively, as manifested by the calculation. In particular,

**Table 5**

Calculated branching ratios for  $J/\psi(\psi', \psi(3770)) \rightarrow \gamma P$  based on the VMD model. Experimental data from PDG 2010 [4] for  $J/\psi$  and  $\psi(3770)$  decays and from BESIII [3] for  $\psi'$  decays are included as a comparison. The phase angles are fixed in such a way that the theoretical results can best describe the central values of the experimental data.

$\gamma P$	$J/\psi \rightarrow \gamma P$		$\psi' \rightarrow \gamma P$		$\psi(3770) \rightarrow \gamma P$	
	Experiment	Theory	Experiment	Theory	Experiment	Theory
$\gamma\pi^0$	$(3.49^{+0.33}_{-0.30}) \times 10^{-5}$	$(1.64 \sim 2.04) \times 10^{-5}$	$(1.58 \pm 0.40 \pm 0.13) \times 10^{-6}$	$(0.66 \sim 1.15) \times 10^{-7}$	$< 2 \times 10^{-4}$	$3.25 \times 10^{-9}$
$\gamma\eta$	$(1.104 \pm 0.034) \times 10^{-3}$	$(1.05 \sim 1.06) \times 10^{-3}$	$(1.38 \pm 0.48 \pm 0.09) \times 10^{-6}$	$(1.39 \sim 1.53) \times 10^{-6}$	$< 1.5 \times 10^{-4}$	$7.95 \times 10^{-7}$
$\gamma\eta'$	$(5.28 \pm 0.15) \times 10^{-3}$	$5.20 \sim 5.22 \times 10^{-3}$	$(1.26 \pm 0.03 \pm 0.08) \times 10^{-4}$	$(1.14 \sim 1.19) \times 10^{-4}$	$< 1.8 \times 10^{-4}$	$1.64 \times 10^{-6}$

it shows that both mechanisms are crucial for our understanding of the observed branching ratio patterns.

The successful account of the observed branching ratio patterns for  $J/\psi(\psi') \rightarrow \gamma P$  in the VMD model has an important implication of the hadronic decay mechanisms for  $J/\psi(\psi') \rightarrow VP$ . It shows that the “puzzling” radiative decay patterns in  $J/\psi(\psi') \rightarrow \gamma P$  have direct connections with the hadronic decay mechanisms, i.e.  $J/\psi(\psi') \rightarrow VP$ , instead of some other abnormal processes. As a consequence, it will guide our further investigations of the transitions of  $J/\psi(\psi') \rightarrow VP$ , and impose constraints on processes such as illustrated by Fig. 1. For instance, the hadronic part of Fig. 1(c) is found to be an important non-perturbative QCD mechanism that contributes predominantly in  $\psi' \rightarrow J/\psi\eta$  and  $J/\psi\pi^0$  [31,32]. As pointed out recently in a series of papers on the subject of non-perturbative transition mechanisms in charmonium decays [14,20,31–35], such intermediate meson loop transitions would be a natural mechanism for evading the pQCD helicity selection rule and explaining the “ $\rho\pi$  puzzle” in  $J/\psi(\psi') \rightarrow VP$ .

#### 4. Summary

In brief, with the available data for  $J/\psi(\psi') \rightarrow VP$ , we show that the VMD model is still useful for our understanding of the newly measured branching ratios for  $J/\psi(\psi') \rightarrow \gamma P$  in association with the  $\eta_c$ – $\eta(\eta')$  mixings via the axial gluonic anomaly. Importance of such a contribution has not been recognized before. In particular, we stress that the intermediate vector charmonia can have significant contributions via e.g.  $\psi' \rightarrow J/\psi\eta \rightarrow \gamma\eta$ . We show that these two mechanisms behave differently in  $J/\psi$  and  $\psi' \rightarrow \gamma P$ , and can be understood by state transition selection rules. We also emphasize that the consistency between  $J/\psi(\psi') \rightarrow \gamma P$  and  $VP$  demonstrated in this work would impose important constraints on the non-pQCD mechanisms in  $J/\psi(\psi') \rightarrow VP$ . It would be useful for our final understanding of the long-standing “ $\rho\pi$  puzzle” in  $J/\psi(\psi') \rightarrow VP$ .

#### Acknowledgements

The author thanks useful discussions with H.-N. Li, X.-Q. Li, and H.-W. Ke. This work is supported, in part, by the National Natural Science Foundation of China (Grant No. 11035006), Chinese Academy of Sciences (KJCX2-EW-N01), and Ministry of Science and Technology of China (2009CB825200).

#### References

- [1] T.K. Pedlar, et al., CLEO Collaboration, Phys. Rev. D 79 (2009) 111101, arXiv:0904.1394 [hep-ex].
- [2] C. Amsler, et al., Particle Data Group, Phys. Lett. B 667 (2008) 1.
- [3] M. Ablikim, et al., BESIII Collaboration, Phys. Rev. Lett. 105 (2010) 261801, arXiv:1011.0889 [hep-ex];  
L.L. Wang (for BESIII Collaboration), talk given at The 4th International Workshop on Charm Physics – Charm 2010, 2010, Beijing.
- [4] K. Nakamura, et al., Particle Data Group, J. Phys. G 37 (2010) 075021.
- [5] V.A. Novikov, M.A. Shifman, A.I. Vainshtein, V.I. Zakharov, Nucl. Phys. B 165 (1980) 55.
- [6] K.T. Chao, Nucl. Phys. B 335 (1990) 101.
- [7] T. Feldmann, P. Kroll, B. Stech, Phys. Lett. B 449 (1999) 339, arXiv:hep-ph/9812269.
- [8] A. Ali, J. Chay, C. Greub, P. Ko, Phys. Lett. B 424 (1998) 161.
- [9] A. Petrov, Phys. Rev. D 58 (1998) 054004.
- [10] T.H. Bauer, R.D. Spital, D.R. Yennie, F.M. Pipkin, Rev. Mod. Phys. 50 (1978) 261; T.H. Bauer, R.D. Spital, D.R. Yennie, F.M. Pipkin, Rev. Mod. Phys. 51 (1979) 407, Erratum.
- [11] T. Bauer, D.R. Yennie, Phys. Lett. B 60 (1976) 169.
- [12] G. Li, Q. Zhao, C.H. Chang, J. Phys. G 35 (2008) 055002, arXiv:hep-ph/0701020.
- [13] Q. Zhao, G. Li, C.H. Chang, Phys. Lett. B 645 (2007) 173, arXiv:hep-ph/0610223.
- [14] Y.J. Zhang, G. Li, Q. Zhao, Phys. Rev. Lett. 102 (2009) 172001, arXiv:0902.1300 [hep-ph].
- [15] Q. Zhao, Nucl. Phys. B (Proc. Suppl.) 207–208 (2010) 347, arXiv:1012.2887 [hep-ph].
- [16] S.J. Brodsky, G.P. Lepage, Phys. Rev. D 24 (1981) 2848.
- [17] V.L. Chernyak, A.R. Zhitnitsky, Nucl. Phys. B 201 (1982) 492; V.L. Chernyak, A.R. Zhitnitsky, Nucl. Phys. B 214 (1983) 547, Erratum.
- [18] V.L. Chernyak, A.R. Zhitnitsky, Phys. Rep. 112 (1984) 173.
- [19] X.H. Mo, C.Z. Yuan, P. Wang, High Energy Phys. Nucl. Phys. 31 (2007) 686, arXiv:hep-ph/0611214.
- [20] Q. Zhao, G. Li, C.H. Chang, Chinese Phys. C 34 (2010) 299, arXiv:0812.4092 [hep-ph].
- [21] C. Amsler, F.E. Close, Phys. Lett. B 353 (1995) 385; C. Amsler, F.E. Close, Phys. Rev. D 53 (1996) 295.
- [22] F.E. Close, A. Kirk, Phys. Lett. B 483 (2000) 345.
- [23] F.E. Close, Q. Zhao, Phys. Rev. D 71 (2005) 094022, arXiv:hep-ph/0504043.
- [24] C.E. Thomas, JHEP 0710 (2007) 026, arXiv:0705.1500 [hep-ph].
- [25] R. Escribano, J. Nadal, JHEP 0705 (2007) 006, arXiv:hep-ph/0703187.
- [26] H.Y. Cheng, H.N. Li, K.F. Liu, Phys. Rev. D 79 (2009) 014024, arXiv:0811.2577 [hep-ph].
- [27] V. Mathieu, V. Vento, Phys. Lett. B 688 (2010) 314, arXiv:1003.2119 [hep-ph].
- [28] A. Seiden, H.F.W. Sadrozinski, H.E. Haber, Phys. Rev. D 38 (1988) 824.
- [29] M. Ablikim, et al., BESIII Collaboration, arXiv:1012.1117 [hep-ex].
- [30] J.L. Rosner, Phys. Rev. D 79 (2009) 097301, arXiv:0903.1796 [hep-ph].
- [31] F.K. Guo, C. Hanhart, G. Li, U.G. Meissner, Q. Zhao, arXiv:1008.3632 [hep-ph].
- [32] F.K. Guo, C. Hanhart, U.G. Meissner, Phys. Rev. Lett. 103 (2009) 082003, arXiv:0907.0521 [hep-ph];  
F.K. Guo, C. Hanhart, U.G. Meissner, Phys. Rev. Lett. 104 (2010) 109901, Erratum.
- [33] X.H. Liu, Q. Zhao, Phys. Rev. D 81 (2010) 014017, arXiv:0912.1508 [hep-ph].
- [34] X.H. Liu, Q. Zhao, arXiv:1004.0496 [hep-ph].
- [35] Q. Wang, X.H. Liu, Q. Zhao, arXiv:1010.1343 [hep-ph].